SUPPLEMENTARY INFORMATION

Computational models of the intestinal environment 3. The impact of cholesterol content and pH on mixed micelle colloids

Estelle J.A. Suys[2,3], Dallas B. Warren[2], Christopher J.H. Porter[2,3], Hassan Benameur[4], Colin W. Pouton[2], David K. Chalmers[1]**

[1]Medicinal Chemistry and [2]Drug Delivery, Disposition and Dynamics, [3]ARC Centre of Excellence in Convergent Bio-Nano Science and Technology, Monash Institute of Pharmaceutical Sciences, Monash University, 381 Royal Pde Parkville, Victoria 3052, Australia. [4]Capsugel Research & Development, Parc d'Innovation, Strasbourg, France.

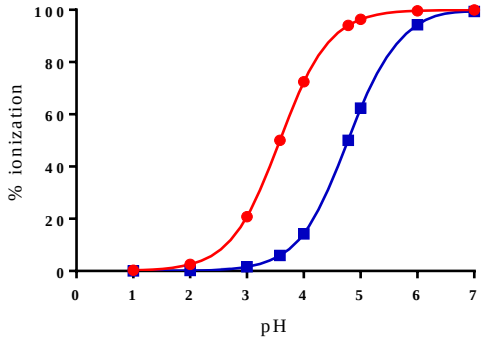

Figure S1. Theoretical titration curves for GDX (●) and OA (■) constructed using the Henderson-Hasselbach equation based on intrinsic pKa values of 3.58[1] and 4.78[2, 3] for GDX and OA, respectively.

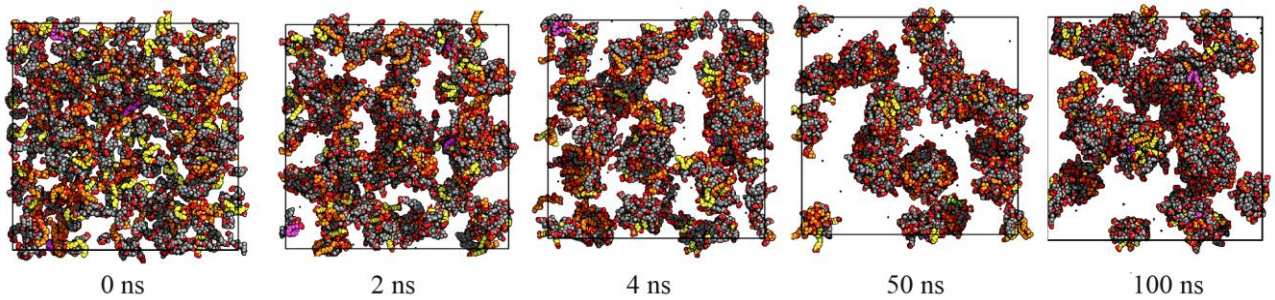

Figure S2. Example of the aggregation process of GDX, LPC and OA at pH 6 in a system without cholesterol (simulation 11). Coloring: grey for GDX, orange for LPC, pink for OA, yellow for OLAT and red for oxygen atoms. Water has been omitted.

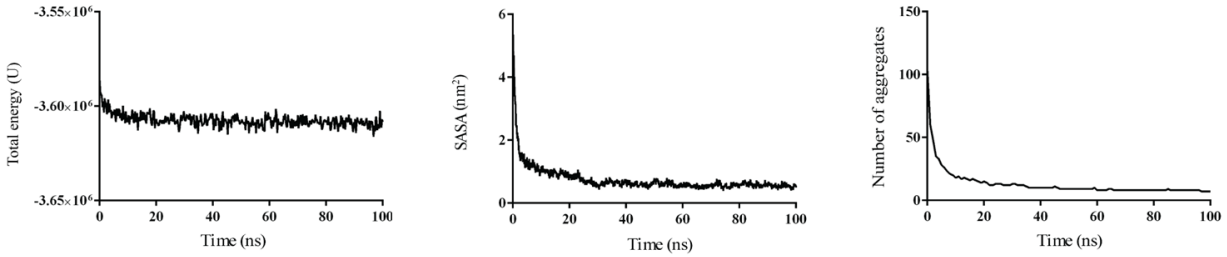

Figure S3. Graphs showing (left) the total energy ($kJ \cdot mol^{-1}$), (centre) the SASA per cholesterol residue (nm^2) and (right) the total number of aggregates for simulation **8** as a function of time (100 ns).

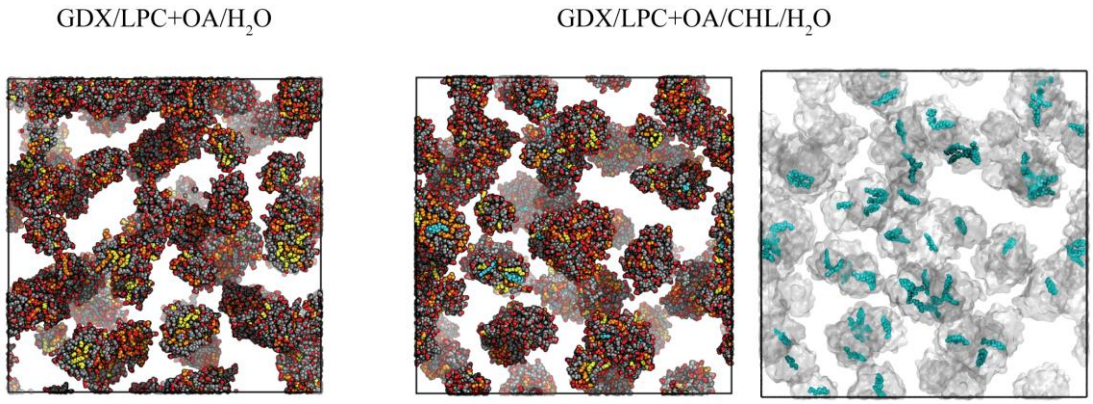

Figure S4. Large-scale simulation of digested bile models at pH 7 after 100 ns. The colours for the residues are: grey for GDX, orange for LPC, pink for OA, yellow for OLAT, light blue for CHL and red for oxygen atoms. The box indicates the periodic cell. Water is not displayed.

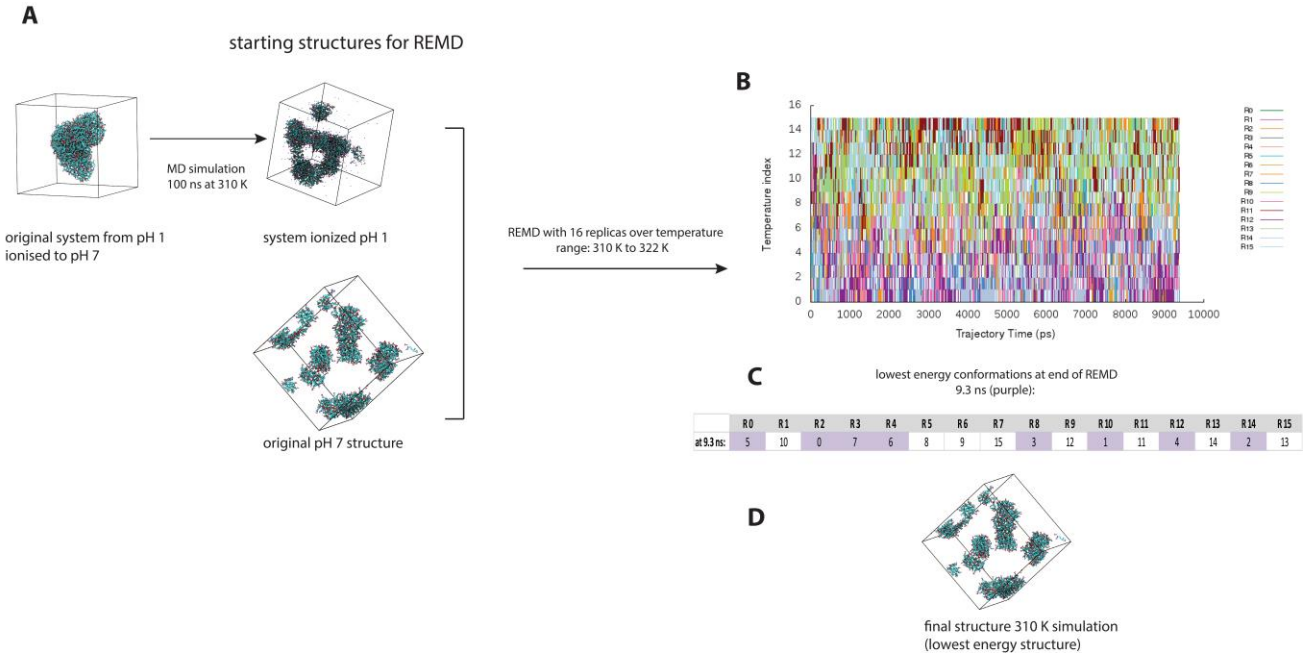

Figure S5. Workflow of the REMD simulation. (A) The large aggregate, obtained from a simulation run at pH 1, was ionised to pH 7 and an intial 100ns simulation was run, producing the top structure shown. A 'small aggregate' model was taken from a pH 7 simulation (bottom) (B). An REMD simulation (temperature range 310 K to 325 K) using 16 parallel simulations was run using 8 large aggregate and 8 small aggregate structurs. Panel B shows the diffusion of replicas during REMD at different temperatures. (C) After temperature replica-exchange, 7 of the 8 lowest energy conformations were found to be small aggregate structures, showing that the small aggregate structure is most stable at 310 K. (D) The 310 K structure (lowest energy) is shown.

Table S1. Spatial distribution probability cut-offs of the atoms, used for generating probability surfaces around GDX(H) as reference molecule for the systems with and without cholesterol (**Error! Reference source not found.**5) at pH 1 and pH 7.

Molecular species	**Spatial distribution probability**			
	C12	C8	P1	C1
LPC		15.79	32.43	
OLE/OLAT	15.96			19.88

Table S2. Spatial distribution probabilities of the atoms, used for generating probability surfaces around cholesterol as reference molecule (5).

Molecular species	**Spatial distribution probability**			
	C19	C16	C14	OW
GDX/GDXH	17.00			
LPC			33.16	
OLE/OLAT		31.50		
Water				9.22

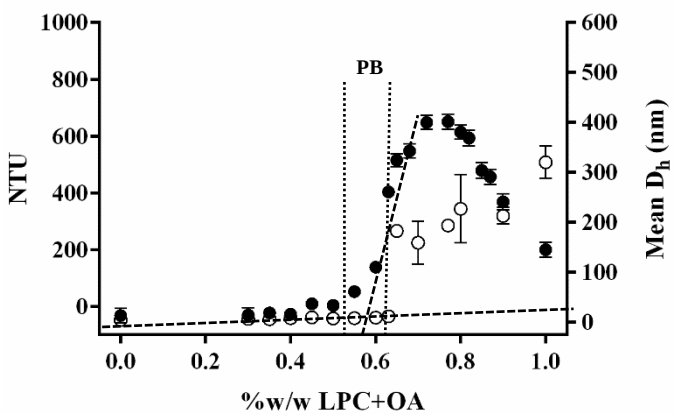

Figure S6. Micelle-vesicle phase boundary determination based on nephelometry (●) and DLS measurements (displayed as mean hydrodynamic diameter, D_h) (○) for 1 % w/w at pH 6 for the system without cholesterol, error bars plotted as SD. Light scattering and turbidity data are plotted versus the mass fraction of digested lipid content (mass fraction of bile salt, GDX, and buffer solution is not displayed). Turbidity data are displayed in arbitrary Nephelometric Turbidity Units (NTU). The dashed lines shows the best fit for the micellar (horizontal line) and vesicular regions (vertical, angled line). The phase boundary (PB) is represented as the range between the dotted lines at the intersection between the two slopes.

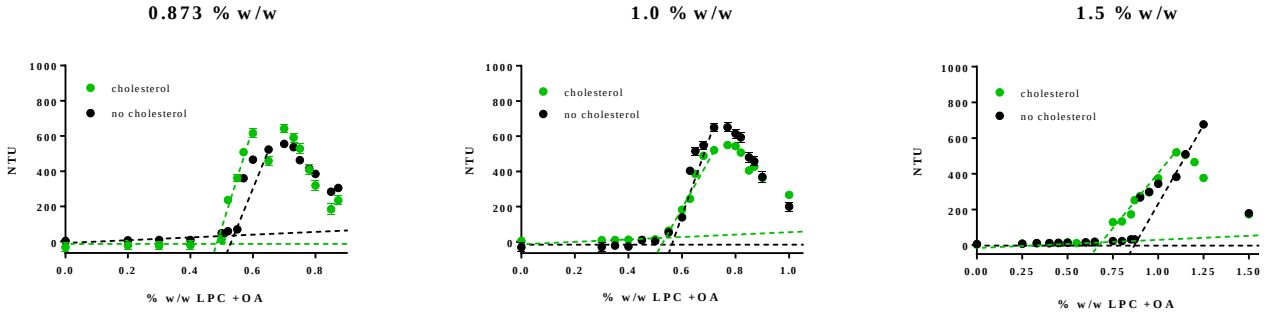

Figure S7. Nephelometry measurements displayed versus weight fraction of equimolar LPC+OA at pH 6 at 0.873, 1.0 and 1.5 % w/w GDX/LPC+OA, for the systems with cholesterol (green) and without cholesterol (black). The weight fraction of GDX and buffer is not displayed. The dashed lines represent best fit of the micellar and vesicular region of the turbidity data (phase boundary) at both pH values.

1. Josephson, B. A. The dissociation constants of bile acid. *Biochem. Z.* **1933,** *263*, 428-443.
2. Cistola, D. P.; Hamilton, J. A.; Jackson, D.; Small, D. M. Ionization and phase behavior of fatty acids in water: application of the Gibbs phase rule. *Biochemistry* **1988,** *27* (6), 1881-1888.
3. Spector, A. A. Fatty acid binding to plasma albumin. *J. Lipid Res.* **1975,** *16* (3), 165-179.